Processing and Photocatalytic Properties of Transparent 12 Tungsto(VI) Phosphoric Acid−TiO_2 Hybrid Films

Sayaka Yanagida,[†] Akira Nakajima,*[,†] Takayoshi Sasaki,[‡] Yoshikazu Kameshima,[†] and Kiyoshi Okada[†]

Department of Metallurgy and Ceramic Science, Tokyo Institute of Technology, 2-12-1 O-okayama, Meguro-ku, Tokyo 152-8552, Japan, and National Institute of Materials Science, 1-1 Namiki, Tsukuba, Ibaraki 305-0044, Japan

Received January 17, 2008

Using the layer-by-layer method, 12 tungsto(VI) phosphoric acid (PW_{12}) and TiO_2 hybrid thin films were prepared. In 2-propanol decomposition, two-bilayer thin films (ca. 15 nm) showed more rapid decomposition than control TiO_2 and PW_{12} films under both UV and visible light illumination. Visible light illumination was required for continuous 2-propanol decomposition. Photocatalytic decomposition activity depends on the number of bilayer coatings, the top coating, and the organic compounds for decomposition. On the basis of the wavelength dependence of the hybrid thin films, a reaction scheme for this system was discussed.

I. Introduction

For environmental purification, TiO_2 is a well-known photocatalyst material.[1] Electron and hole pairs are generated when UV is illuminated on TiO_2. They respectively reduce and oxidize adsorbed molecules on the TiO_2 surface, thereby producing radical species such as $^{\bullet}OH$ and O_2^-. These radicals and surface holes can decompose most organic compounds or even bacteria to H_2O and CO_2. To date, numerous studies have examined improvement of the decomposition activity of TiO_2 photocatalyst against various target compounds by metal modification[2] or combination with other materials.[3–5]

Heteropolyacids (HPAs) are a series of inorganic clusters: they are polymeric oxoanions that consist of more than two kinds of oxoanions. Their general formulas are presented as $[X_xM_mO_p]^{n-}$ (M = W, Mo, V, Nb, Cr, and Ta), where X is generally called a heteroatom. Especially, Keggin-type HPAs ($[XM_{12}O_{40}]^{n-}$) are well investigated and applied within the chemical industry because of their strong oxidation power and high stability in low pH conditions. [6,7] This type of HPA is widely used as a thermal catalyst for epoxidation, hydration, asymmetric syntheses, oxidation, and polymerization.[8,9] A notable characteristic of Keggin-type solid HPAs (Na salt and hydrogen-form Keggin anions) is the absorption of a large amount of some polar molecules. Some alcohols, ketones, and amines[10] are absorbed and diffused into this type of solid HPA. For that reason, in some cases, catalytic reactions occur not only on the surface but also inside of Keggin-type solid HPAs. The resultant so-called bulk-type reaction differs from a surface reaction.[11]

Keggin-type HPAs are also known as photocatalysts.[12,13] Electrons are promoted from an orbital of oxygen to that of metal atom (such as from O 2p to W 3d) when UV is illuminated to Keggin-type HPAs. This oxygen-to-metal charge transfer engenders electron charge separation. In the photocatalytic reaction, generated holes oxidize organic molecules;[14] then HPAs are reduced. The reduced HPAs absorb visible light of a restricted wavelength range because this absorption is attributable to its d−d transition or IV transition.[15]

Photocatalytic reduction activity of $H_3PW_{12}O_{40}$, a Keggin-type HPA (hereafter denoted as PW_{12})−TiO_2 hybrid system, was examined in aqueous media.[16−18] The reduction potential of PW_{12} (+0.22 V vs NHE) is lower than the conduction band level of TiO_2 (−0.5 V vs NHE). Conse-

* Corresponding author. Tel.: +81-3-5734-2525. Fax: +81-3-5734-3355. E-mail: anakajim@ceram.titech.ac.jp.
[†] Tokyo Institute of Technology.
[‡] National Institute of Materials Science.

(1) Fujihira, M.; Satoh, Y.; Osa, T. *Nature* **1981**, *293*, 206.
(2) Sato, S.; White, J. M. *Chem. Phys. Lett.* **1980**, *72*, 83.
(3) Yamashita, H.; Anpo, M. *Curr. Opin. Solid State Mater. Sci.* **2004**, *7*, 471.
(4) Nozawa, M.; Tanigawa, K.; Hosomi, M.; Chikusa, T.; Kawada, E. *Water Sci. Technol.* **2001**, *44* (9), 127.
(5) Nakajima, A.; Takakuwa, K.; Kameshima, Y.; Hagiwara, M.; Sato, S.; Yamamoto, Y.; Yoshida, N.; Watanabe, T.; Okada, K. *J. Photochem. Photobiol. A: Chem.* **2006**, *177*, 94.
(6) Borrás-Almenar, J. J.; Coronado, E.; Müller, A.; Pope, M. *Polyoxometalate Molecular Science*; Kluwer Academic Publishers: Dordrecht, 2003.
(7) Mizuo, N.; Misono, M. *Chem. Rev.* **1998**, *98*, 199.
(8) Kozhevnikov, I. V. *Chem. Rev.* **1998**, *98*, 171.
(9) Mitsutani, A. *Catal. Today* **2002**, 57.
(10) Okuhara, T.; Kasai, A.; Hayakawa, N.; Misono, M.; Yoneda, Y. *Chem. Lett.* **1981**, 391.
(11) Misono, M. *Mater. Chem. Phys.* **1987**, *17*, 103.
(12) Yamase, T. *Catal. Surv. Asia* **2003**, *7* (4), 203.
(13) Hiskia, A.; Mylonas, A.; Papaconstantinou, A. *Chem. Soc. Rev.* **2001**, *30*, 62.
(14) Hill, C. L.; Bouchard, D. A. *J. Am. Chem. Soc.* **1985**, *107*, 5148.
(15) Yamase, T. *Chem. Rev.* **1998**, *98*, 307.
(16) Park, H.; Choi, W. *J. Phys. Chem. B* **2003**, *107*, 3885.
(17) Yoon, M.; Chang, J. A.; Kim, Y.; Choi, J. R.; Kim, K.; Lee, S. J. *J. Phys. Chem. B* **2001**, *105*, 2539.
(18) Tachikawa, T.; Tojo, S.; Fujitsuka, M.; Majima, T. *Chem. Eur. J.* **2006**, *12*, 3124.

10.1021/cm800167x CCC: $40.75
Published on Web 05/08/2008

quently, HPA acts as an electron scavenger of TiO_2. Reduced PW_{12} (PW_{12}^-) absorbs visible light to form an excited-state PW_{12}^-(PW_{12}^-*). Then it reduces organic compounds such as methyl viologen or methyl orange in water. [17,18] However, to date, all examinations were carried out in aqueous solution. In this work, photocatalytic decomposition activities of PW_{12}−TiO_2 hybrids were investigated in the gaseous phase under various illumination conditions. In this system, a high decomposition rate was expected because of the electron scavenger effect and adsorption of organic molecules by PW_{12}.

Various coatings including self-assembled monolayers or organic−inorganic composites were prepared using the layer-by-layer coating method.[19,20] Advantages of this method are (1) easy processing of a nano-order composite, (2) easy control in coating thickness by changing deposition times, and (3) various available combinations of building blocks. For this study, we prepared transparent TiO_2−PW_{12} hybrid thin films by this method using TiO_2−sol and PW_{12} solution. Subsequently, its photocatalytic behavior was evaluated using the decomposition of gaseous 2-propanol.

II. Experimental Section

II-I. Film Processing. *(a) $(PW_{12}/TiO_2)_n$ Thin Film.* A commercial TiO_2 aqueous suspension (STS-100, 20 wt % concentration; Ishihara Sangyo Kaisha Ltd., Mie, Japan) was used as the starting material. The suspension contains HNO_3 as a stabilizer to maintain a well-dispersed state of anatase nanoparticles. Transmission electron microscope (TEM) observations revealed that the suspension contains monodispersed anatase nanoparticles with dimensions of 5−7 nm. This suspension was diluted with aqueous solutions of reagent-grade HNO_3; then, 0.004−0.4 g dm^{-3} (2, 5, 10, 20, 50 mg/dm^3, 0.1, 0.2, 0.4 g dm^{-3}) suspensions were prepared. Actually, PW_{12} requires low pH (<2) to prevent its hydrolysis.[21] The TiO_2 particles have sufficient positive charge for maintaining a well dispersed state and for layer-by-layer coating using Coulombic attraction with PW_{12} molecules. For those reasons, the pH values of these TiO_2 suspensions were adjusted to 1.5 using HNO_3.

For all experiments, 12 tungsto(VI) phosphoric acid *n*-hydrate (Wako Pure Chemical Industries Ltd., Tokyo, Japan) was used without any purification. This chemical was dissolved into diluted HNO_3 solution; the PW_{12} aqueous solution (0.9 mM, calculated as M = 3399, $PW_{12}O_{40}\cdot 29H_2O$, pH value was adjusted to 1.5) was prepared.

Pure quartz (SiO_2) glass plates (30 mm × 60 mm × 1 mm; Tosoh Corp, Tokyo, Japan) and Si(100) wafers (40 mm × 60 mm × 0.5 mm; Aki Corp., Miyagi, Japan) were used as substrates. After normal cleaning procedures,[22,23] substrates were soaked in a bath of 1:1 methanol/HCl and then concentrated H_2SO_4 for 30 min each. Substrates were soaked in distilled water and ultrasonicated for 10 min. First, these substrates were immersed into PW_{12} solution for 20 min. The substrates' surface is positively charged in acid solution. Therefore, the first layer of PW_{12} molecules was adsorbed on the surface of substrates by Coulombic potential. After immersion, the substrates were rinsed twice using diluted HNO_3 (pH = 1.5) solution to remove excess PW_{12}. Then, the substrates were dried at 60 °C in an oven under air atmosphere for 15 min. Second, PW_{12} coated substrates were immersed into a TiO_2 suspension for 20 min. Then they were rinsed twice with diluted HNO_3. The substrates were dried under the same conditions as those for PW_{12} coating. The PW_{12}−TiO_2 hybrid thin films were prepared by alternate immersion and washing processes. Herein, the PW_{12}−TiO_2 hybrid thin film with *n*-times bilayer deposition is designated as a $(PW_{12}/TiO_2)_n$ hybrid film.

(b) TiO_2 Nanoparticle Thin Film. Control samples were prepared according to a process used in a study by Sasaki et al.[23] The TiO_2 suspension (0.2 g dm^{-3}) was prepared using an identical procedure for $(PW_{12}/TiO_2)_n$ hybrid films. Poly(sodium 4-styrene sulfonate) (PSS, average MW ca. 70 000, 30 wt % aqueous solution; Aldrich Corp.) was used for preparation of control TiO_2 films. A PSS (7 g dm^{-3}) solution was prepared by dissolving a certain mass of PSS in a HNO_3 solution whose pH was 1.5. First, substrates were immersed into the PSS solution for 20 min. They were then rinsed twice with diluted HNO_3 (pH = 1.5). The samples were dried at 60 °C in an oven under air atmosphere. Second, the sample was immersed in a TiO_2 suspension for 20 min and rinsed twice with diluted HNO_3 (pH = 1.5). The samples were dried at 60 °C under an air atmosphere. Then $(PSS/TiO_2)_n$ thin films were obtained by repeating these procedures. After deposition, UV light was illuminated on the samples using a Hg−Xe lamp for 6 h to decompose interlayer PSS. The illumination intensity at the sample surface was 66 mW/cm^2 at λ = 365 nm. Subsequently, $(TiO_2)_n$ samples were obtained.

(c) PW_{12} Thin Film. For preparation of the control PW_{12} thin films, poly(diallyldimethylammonium chloride) (PDDA, typical MW 100 000−200 000, 20 wt % aqueous solution; Aldrich Corp.) was used as a counter polymer. A PDDA (20 g dm^{-3}) solution was prepared by dissolving a certain mass of PDDA in a HNO_3 solution of pH 1.5. First, substrates were immersed into the PW_{12} solution for 20 min. They were then rinsed twice with diluted HNO_3 (pH = 1.5). The samples were dried at 60 °C in an oven under an air atmosphere. Then the sample was immersed in PDDA solution for 20 min and rinsed twice with diluted HNO_3 (pH = 1.5). The samples were dried at 60 °C under an air atmosphere. Subsequently, $(PDDA/PW_{12})_n$ thin films were obtained by repeating these procedures. After deposition, UV light was illuminated onto the samples using a Hg−Xe lamp for 16 h to decompose the interlayer PSS. The illumination intensity at the sample surface was 66 mW/cm^2 at λ = 365 nm. Finally, $(PW_{12})_n$ samples were obtained.

II-2. Evaluation. *(a) Structure and Composition of Thin Films.* Using a UV−vis−NIR scanning spectrophotometer (V-630; Jasco Inc., Tokyo, Japan), UV−vis absorption spectra were evaluated. The infrared spectra of the thin films on the Si substrate were recorded using a Fourier transform infrared (FT-IR) spectrophotometer (8600PC; Shimadzu Corp., Kyoto, Japan). Transmission mode was used with an incidence angle of 75° (Brewster's angle). Reflectance spectra were measured using another UV−vis−NIR scanning spectrophotometer (UV-2400 Shimadzu Corp., Kyoto, Japan) with an integrating sphere. Layer thickness was estimated using a surface profiler (Dektak3; Ulvac Technologies, Inc., Kanagawa, Japan) with a diamond-tipped stylus (r = 12.5 μm). Its vertical resolution was 0.5 nm. The scan length was 5000 μm; data points were 2000. Morphology of the prepared films was evaluated using non-contact-mode of an atomic force microscope (AFM, JSPM 5200; JEOL, Tokyo, Japan). A Pt−Ti coated Si cantilever (force constant: 0.95 N/m) was used for this measurement. The surface chemical composition was measured using X-ray photoelectron spectroscopy (XPS, 5500MC; Perkin-Elmer Phi Co., U.S.A.) with a Mg Kα X-ray line (46.950 eV). The takeoff angle

(19) Iler, R. K. *J. Colloid Interface Sci.* **1966**, *21*, 569.
(20) Decher, G. *Science* **1997**, *277*, 1232.
(21) Kepert, D. L.; Kyle, J. H. *J. Chem. Soc., Dalton* **1978**, 1781.
(22) Wang, Z.-S.; Li, F.-Y.; Huang, C.-H.; Wang, L.; Wei, M.; Jin, L.-P.; Li, N.-Q. *J. Phys. Chem. B* **2000**, *104*, 9676.
(23) Sasaki, T.; Ebina, Y.; Tanaka, T.; Harada, M.; Watanabe, M. *Chem. Mater.* **2001**, *13*, 4661.

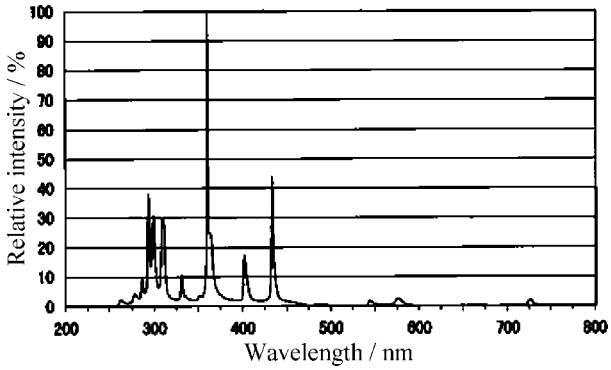

Figure 1. Wavelength spectra of the light source. Reprinted with permission from ref 24. Copyright Hayashi 2000–2006.

was 45°. The binding energy scales were referenced to 284.5 eV, as determined by locations of peaks on the C 1s spectra of hydrocarbon (CH_x) for correcting the deviation.

(b) Photocatalytic Activity. Photocatalytic activity was evaluated according to the decomposition of gaseous 2-propanol (Wako Pure Chemical Industries Ltd.). The $(PW_{12}/TiO_2)_n$ films, the $(PW_{12}/TiO_2)_n$+PW_{12} films, whose top was covered with a PW_{12} layer, the $(TiO_2)_n$ films, and $(PW_{12})_n$ films ($n = 2$ or 6) on glass substrate were used in this experiment. Four sample films were exposed to strong UV light (224 mW/cm^2, 365 nm) before experiments to remove organic compounds adsorbed on the surface. A Pyrex glass vessel (500 mL in volume) with a quartz glass lid was used as a batch reactor. A sample film was set at the center of the vessel. Subsequently, the vessel was sealed, and 2-propanol gas was injected into it. The injected gas amount was equivalent to that for 50 ppm concentration. The vessel was then stored in the dark. During this dark storage, the 2-propanol concentration decreased because of molecules' adsorption on the sample and the vessel surface. The concentration change was monitored using gas chromatography (GC-14A; Shimadzu Corp., Tokyo, Japan). That device was equipped with a flame ionization detector (FID), a methanizer, and a Sunpak-A column (Shimadzu Corp.). The carrier gas was nitrogen; the respective temperatures for the detector and injection port were 230 and 200 °C. The initial column temperature was 70 °C, which was maintained for 2.5 min; the temperature was increased 20 °C/min to 130 °C to peak separation. After adsorption the equilibrium was confirmed, and UV illumination was carried out using a UV Illuminator (LA-410UV-1; Hayashi Watch Works Co. Japan) equipped with a Hg−Xe lamp (MX4010). This light sorce contains several peaks in the 280−450 nm range with the strongest peak at 365 nm (Figure 1).[24] The illumination intensity at the layer surface was 1 mW/cm^2 at 365 nm. The 2-propanol, acetone, and CO_2 concentrations were evaluated every 30 min during 4 h. Two colored glass filters, UV-33 (absorbed UV < 330 nm, Asahi Glass Co. Ltd., Japan) and UV-D33S (absorbed visible light > 400 nm, Asahi Glass) were used to limit the wavelength range of light illumination. In both the UV-limited and vis-limited cases, the illumination intensity was 1 mW/cm^2 at 365 nm. Other experimental conditions were the same as those of the all-light illumination case.

III. Results and Discussion

III-1. Film Processing. Figure 2 presents a schematic illustration of the layer-by-layer method. In an acid solution, the Coulomb force adsorbed negatively charged PW_{12} and positively charged TiO_2 particles with each other. The PW_{12}−TiO_2 bilayer becomes thick through alternate immersion. Figure 3 shows the TiO_2 suspension concentration dependence of the absorbance of the $(PW_{12}/TiO_2)_n$ hybrid film at $\lambda = 248$ nm. The absorbance increased with increasing TiO_2 suspension concentration up to 0.1 g dm^{-3} and then was saturated. On the basis of this result, we determined the concentration of to TiO_2 suspension for film processing to be 0.2 g/L. Subsequent experiments were carried out using this TiO_2 suspension. The absorption change was not remarkable against the withdrawal rate (1−10 mm/s) and the immersion time when it was longer than 20 min.

Figure 4 shows the dependence of UV−vis absorption spectra on the layer number of the $(PW_{12}/TiO_2)_n$ hybrid films. Both PW_{12} and TiO_2 possess absorption bands in UV region.

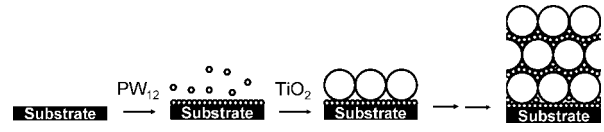

Figure 2. Schematic illustration of self-assembly film preparation.

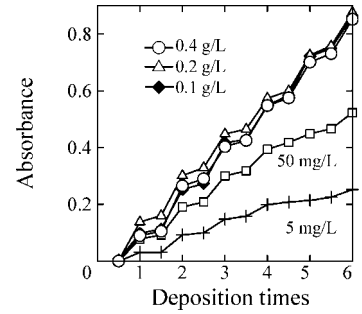

Figure 3. UV absorbance change at $\lambda = 248$ nm.

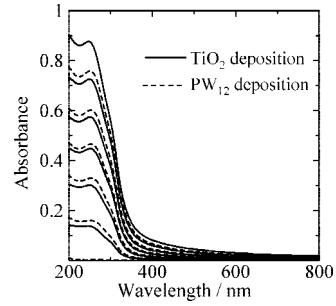

Figure 4. UV−vis absorbance spectra change of the $(PW_{12}/TiO_2)_n$ self-assembly layer. The TiO_2 particle concentration is 0.2 g/dm^3, and the deposition time is 20 min. The solid lines represent spectra of $n = 1$, 2, 3, ... bilayers. The dashed line represents spectra after PW_{12} deposition.

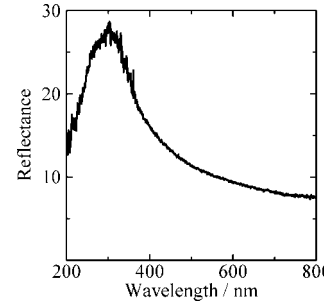

Figure 5. UV−vis reflectance spectrum of the $(PW_{12}/TiO_2)_6$ hybrid film.

(24) http://www.htkgp.co.jp/hwatch/tokuhin/luminar/LA-410UV.html (accessed April 2008).

Therefore, absorbance was increased with both depositions. The spectra for the $(PW_{12}/TiO_2)_6$ hybrid film imply that transmittance in the visible area (λ = 400−780 nm) was higher than 83%. An average increment in absorbance was 0.129 for the TiO_2 particle layer and 0.026 for the PW_{12} layer at λ = 248 nm. An average of bilayer absorbance 0.155 was equal to the sum of these values. Figure 5 depicts reflectance spectra of the $(PW_{12}/TiO_2)_6$ hybrid film. Using absorbance and reflectance spectra, the TiO_2 packing density is calculable. Based on Sasaki's method,[23,25] real absorbance is represented as

$$T = 1 - R - A$$

where T is the transmittance, R is the reflectance, and A is the damping ratio attributable to actual absorbance. For the $(PW_{12}/TiO_2)_6$ hybrid film, the apparent absorbance was 0.774 (= 0.129 × 6). This value is converted to T = 0.168. Based on the reflectance spectra shown in Figure 5, R is obtainable as 0.228 at λ = 248 nm. Therefore, the value of A is calculated as 0.604 (= 1 − 0.168 − 0.228). Assuming no multiple refraction at the interface and no intensity loss through internal defects, the actual incident beam into the sample is presented as (1 − R). Consequently, the actual transmittance (T/(1 − R)= 0.168/0.772) is calculated as 0.218. This value is convertible to an absorbance value of 0.662 (= −log 0.218). The average absorbance per TiO_2 layer was 0.055 (= 0.218/12) because six layers exist on both sides of substrate glass plate. Because the TiO_2 suspension exhibits a Lambert−Beer relationship,[24] the molar extinction coefficient (ε) was obtainable from experimental data as 3.90 × 10^3 mol^{-1} dm^3 cm^{-1} at λ = 248 nm. Assuming the same ε on a TiO_2 particle in the thin film layer and 6-nm particle layer thickness (= TiO_2 particle diameter), the TiO_2 amount per unit layer can be estimated roughly from the Lambert−Beer equation ($A = \varepsilon bc$) as

$$0.055 = 3.90 \times 10^3 \times 6.0 \times 10^{-7} \times c$$

In the previous equation, c = 24 mol/dm^{-3}; it can be converted to 1.1 × 10^{-6} g cm^{-2}. The TiO_2 amount is calculable using the following equation if TiO_2 particles are packed by the closest packing in a 2D plane.[25]

$$m = \frac{4}{3}\pi r^3 \rho / S_{UC}$$

$$S_{UC} = d^2 \sin 120°$$

In the previous two equations, d and r respectively represent the particle diameter and radius and ρ is the density of TiO_2 (for anatase, 3.89 g/cm^{-3}). In addition, S_{UC} is the unit cell area of the closest packing in the 2D plane (Figure 6). The m value is calculated as 1.41 × 10^{-6} when r = 3 nm. Comparing the estimated value between experimental data and theoretical particle packing, the packing density of the film is estimated as 78% of the closest particle packing. This density is attributable to the repulsion force between TiO_2 particles or the imbalance of charge density in the film.

Figure 7a shows the dependence of UV−vis absorption spectra on the layer number of the $(PSS/TiO_2)_n$ hybrid films.

(25) Wang, Z-S.; Sasaki, T.; Muramatsu, M.; Ebina, Y.; Tanaka, T.; Wang, L.; Watanabe, M. *Chem. Mater.* **2003**, *15*, 807.

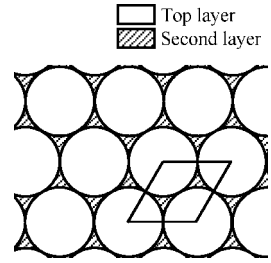

Figure 6. Schematic illustration of the closest 2D packing.

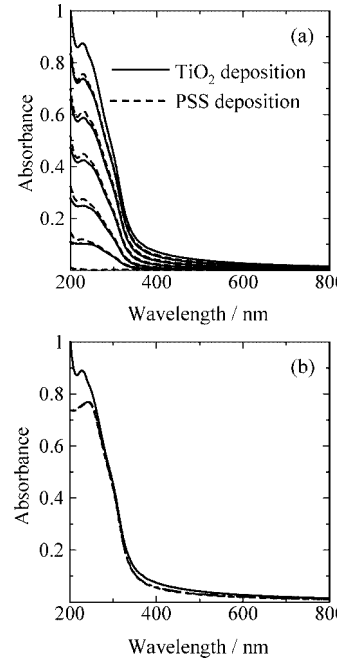

Figure 7. UV−vis absorbance spectra change of the $(PSS/TiO_2)_n$ self-assembly layer. (a) Layer growth with deposition times. The particle concentration was 0.2 g/dm^3; the soaking time was 20 min. Solid lines represent bilayer spectra. Dashed lines represent spectra after PW_{12} deposition. (b) $(PSS/TiO_2)_6$ sample absorbance spectra before and after UV illumination.

Average increments of a TiO_2 layer and a PSS layer at λ = 228 nm were, respectively, 0.133 and 0.024. These values agree with those presented in a previous work.[25] Figure 7b presents the UV−vis absorption spectra of the $(PSS/TiO_2)_6$ hybrid film before and after UV illumination. The PSS layers were decomposed by the TiO_2 photocatalyst; the absorbance in the wavelength range of less than 300 nm decreased. This absorbance change was saturated after 2 h of illumination. For this study, we therefore adopt this illumination time (2 h) for processing of the control $(TiO_2)_6$ film.

Figure 8 a shows the dependence of UV−vis absorption spectra on the layer number of the $(PW_{12}/PDDA)_n$ hybrid films. Actually, PDDA only absorbed near 200 nm UV in this range, so the λ = 260 nm peak was attributed to PW_{12} absorption. Figure 8 b shows UV−vis absorption spectra before and after UV illumination. After illumination, absorbance by PDDA (mainly λ < 250) disappeared. It is probably attributable to PDDA decomposition by PW_{12} photocatalyst. The slight increase of PW_{12} peaks is attributable to the difference of the supporting material.[26]

Figure 9 shows the height profile of the $(PW_{12}/TiO_2)_2$ hybrid film. Each coating of this film was performed by

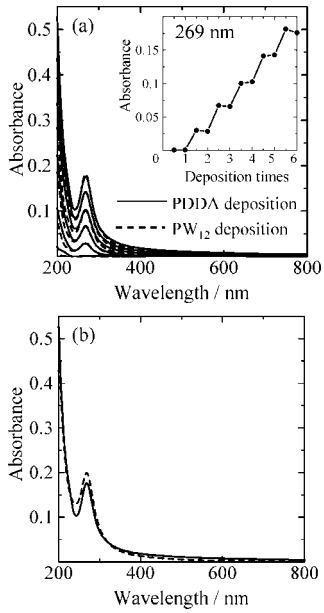

Figure 8. UV−vis absorbance spectra change of the $(PW_{12}/PDDA)_n$ self-assembly layer. (a) Layer growth with deposition times. Solid lines represent bilayer spectra with absorbance change at 269 nm (inset figure). Dashed lines represent spectra after PW_{12} deposition. (b) $(PW_{12}/PDDA)_6$ sample absorbance spectra before and after UV illumination.

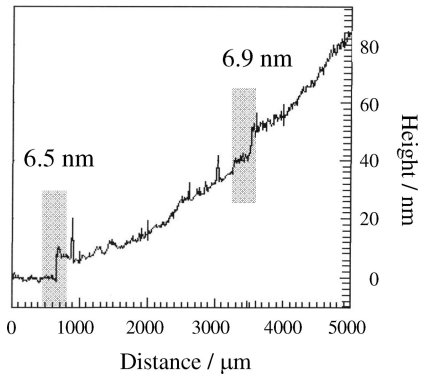

Figure 9. 2D-height profile of the $(PW_{12}/TiO_2)_2$ hybrid film.

displacing the coating position around 3 mm from the former coating. A curved baseline was attributable to the swelling of substrate. Two step structures were visible at distances of 700 μm and 3700 μm. Step heights at these positions are 6.5 and 6.9 nm; these values are almost equivalent to the sum of a TiO_2 particle (6 nm) and PW_{12}diameter (1.12 nm).[27] This result clarifies that TiO_2 adsorption is likely to take place in a single layer. Some sharp peaks in the profile might be particles adsorbed on the first layer. However, the radius of the diamond-tipped stylus (12.5 μm) is too large to measure gaps separating particles. Particle packing can not be discussed from these data. Figure 10 presents the microstructure of the first bilayer on the Si substrate. The Si surface was covered with TiO_2 particles even after washing. Most of the TiO_2 layer was of about 6−7 nm thickness.

Figure 11 portrays IR spectra of the $n = 5$ bilayer hybrid films on a Si substrate: $H_3PW_{12}O_{40}$ (KBr method). Keggin-

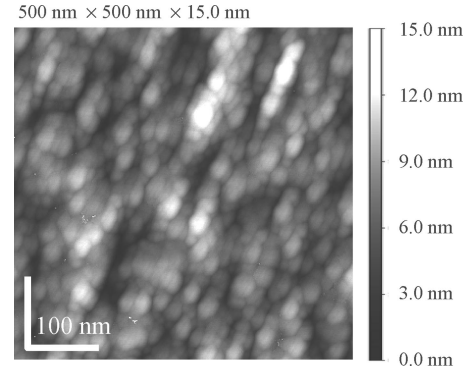

Figure 10. AFM image of the $(PW_{12}/TiO_2)_1$ film on the Si substrate.

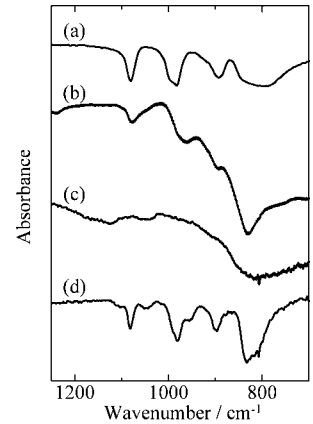

Figure 11. IR spectra of the starting material ($H_3PW_{12}O_{40}$) and composites: (a) $H_3PW_{12}O_{40}$ (KBr method), (b) $(PW_{12}/TiO_2)_5$ film on the Si substrate, (c) $(PSS/TiO_2)_5$ film on the Si substrate after UV illumination, and (e) $(PW_{12}/PDDA)_5$ film on the Si substrate after illumination.

type HPA exhibits characteristic absorbance of 700−1200 cm^{-1}. If PW_{12} is hydrolyzed and a Keggin structure is decomposed, a P−O stretching peak (1080 cm^{-1}) should be split into two peaks.[28] The single 1080 cm^{-1} peak in the $(PW_{12}/TiO_2)_5$ hybrid film spectra indicates that the Keggin structure remains in the film.

Our XPS measurements revealed that the surface atomic ratios between W(4d)/Ti(2d) on the $(PW_{12}/TiO_2)_2$+PW_{12} film and the $(PW_{12}/TiO_2)_3$ hybrid film were, respectively, 0.7 and 0.1. We can calculate the surface W/Ti ratio of the film by assuming the following condition when PW_{12} is the top layer: (1) TiO_2 nanoparticle and PW_{12} ion are a 6-nm sphere (ρ = 3.89 g /cm^3) and a 1-nm sphere (ρ = 9.12 g /cm^3, as calculated from $\rho_{PW12} = (M_{PW12}/N_A)/[(4/3)\pi r^3]$, where N_A is Avogadro's constant); (2) the PW_{12} top layer has a two-dimensional closed packing hexagonal structure; (3) the second layer is filled completely with TiO_2; (4) electrons were emitted from the constant depth z; and (5) composition depends on the surface coverage ratio of TiO_2 and PW_{12}. Considering the size difference between TiO_2 and PW_{12}, this assumption is reasonable. On the basis of the assumptions described above, the surface coverage is represented as follows.

(26) Edward, J.; Thiel, C. Y.; Benac, B.; Knifton, J. F. *Catal. Lett.* **1998**, *51*, 77.
(27) Kurucseav, T.; Sargesoan, M.; West, B. O. *J. Phys. Chem.* **1957**, *61*, 1567.
(28) Edwards, J. C.; Thiel, C. Y.; Benac, B.; Knifton, J. F. *Catal. Lett.* **1998**, *51*, 77.

$$f_{PW12} = \frac{\pi r^2}{S_{UC}}$$

$$f_{TiO2} = 1 - \frac{\pi r^2}{S_{UC}}$$

In those equations, f represents the surface coverage of PW_{12} and TiO_2 and r is the PW_{12} radius. Therefore,

$$W/Ti = \frac{f_{PW12} \times z \times \frac{\rho_{PW12}}{M_{PW12}} \times 12}{f_{TiO2} \times z \times \frac{\rho_{TiO2}}{M_{TiO2}}}$$

The surface W/Ti ratio is calculated as 0.77 when PW_{12} is the top layer. This value is almost identical to the value from XPS. When TiO_2 is the top layer with two-dimensional closed packing hexagonal structure, W/Ti is estimate as 0.081. The calculated values are less than the experimental value of 0.1, suggesting that TiO_2 packing is not closed, which also well agrees with the UV data.

III-2. Photocatalytic Activity. Both TiO_2 and PW_{12} can decompose gaseous 2-propanol by photocatalytic reaction. The decomposition pathway of this reaction is studied extensively.[29−31] The molecule of gaseous 2-propanol is initially decomposed into acetone and finally decomposed to H_2O and CO_2. The photocatalytic decomposition rate of acetone by TiO_2 photocatalyst is much slower than that of 2-propanol because of displacement by water vapor from the TiO_2 surface[32] and because of the reaction rate difference from $^{\bullet}OH$ radical.[33]

Figure 12 portrays the change of the concentrations of 2-propanol and acetone during UV illumination for the $(PW_{12}/TiO_2)_2$ hybrid film, the $(PW_{12}/TiO_2)_2$+PW_{12} film (PW_{12} was the top layer), the $(TiO_2)_2$ film (photodecomposed $(PSS/TiO_2)_2$ film), and the $(PW_{12})_2$ film (photodecomposed $(PW_{12}/PDDA)_2$. In that figure, C_0 represents the initial concentration after 2.5 h of dark storage in the case of 2-propanol and CO_2. The initial concentration was 26−28 ppm at the beginning of illumination. According to blank tests, most of the 2-propanol that had decreased during dark storage was adsorbed on the glass cell. The thin film sample had a small surface area. For that reason, comparison of adsorption amounts among samples was difficult. For acetone, $C/C_0 = 1$ was defined as the initial concentration of 2-propanol. Comparing the 2-propanol decomposition rate, the hybrid thin films exhibited higher photocatalytic activity despite their small film thickness (<15 nm). The $(PW_{12})_2$ thin film exhibited quite low photocatalytic activity. The sum of the decomposition amount by $(PW_{12})_2$ and $(TiO_2)_2$ films was less than that by the $(PW_{12}/TiO_2)_2$ hybrid thin film, which indicated that some interaction exists between PW_{12} and TiO_2

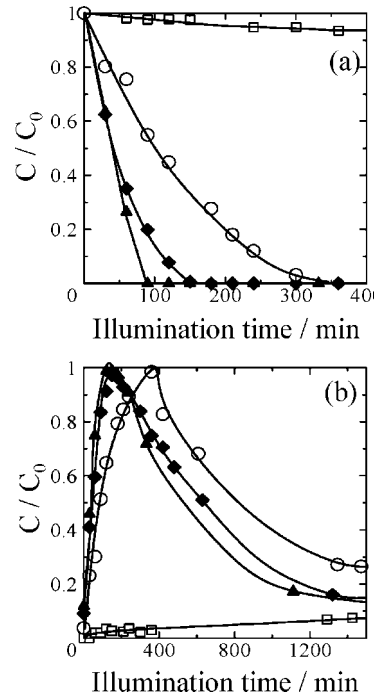

Figure 12. 2-Propanol and acetone concentration change during UV illumination: ○, $(TiO_2)_2$; ♦, $(PW_{12}/TiO_2)_2$; ▲, $(PW_{12}/TiO_2)_2$ covered with PW_{12} layer; and □, $(PW_{12})_2$.

to hasten 2-propanol decomposition. The initial 2-propanol decomposition rate of $(PW_{12}/TiO_2)_2$+PW_{12} was almost equal to that of $(PW_{12}/TiO_2)_2$ despite different TiO_2 surface coverages. Photocatalytic decomposition activity on the gaseous compound that adsorbs on the surface of TiO_2 usually depends on the TiO_2 surface area.[34]

After 30 h of decomposition, the increment of CO_2 concentration (ΔCO_2) was about 150 ppm. The injected 2-propanol amount in the vessel corresponded to 50 ppm. Consequently, nearly three times the amount of CO_2 should be generated. Therefore, 2-propanol was expected to be decomposed completely.

Decomposition experiments were carried out with $n = 6$ samples to investigate the decomposition rate dependence on layer thickness. Figure 13 shows the concentration change of 2-propanol and acetone during UV illumination. The activity of the TiO_2 control sample was increased with increasing layer thickness, which is expected to reflect the increasing number of photogenerated holes and resultant radical species. On the other hand, the $(PW_{12}/TiO_2)_6$+PW_{12} film exhibited almost the same 2-propanol decomposition rate as the $n = 2$ sample. These results indicated that the bottom or inner part of the $n = 6$ sample did not contribute to decomposition of 2-propanol. In other words, only the top part, for example, one or two layers from the surface, was the reaction field on 2-propanol decomposition. Misono reported that a PW_{12} cluster absorbs an integral multiple of organic molecules.[11] In the case of the $(PW_{12})_6$ film, the 2-propanol concentration decreased gradually with time; however, the acetone concentration was almost identical to

(29) Harvey, P. R.; Rudham, R.; Ward, S. *J. Chem. Soc., Faraday Trans.* **1983**, *1*, 1381.
(30) Ohko, Y.; Hashimoto, K.; Fujishima, A. *J. Phys. Chem. A* **1997**, *101*, 8057.
(31) Mylonas, A.; Hiskia, A.; Androulaki, E.; Dimotikali, D.; Papaconstantinou, E. *Phys. Chem. Chem. Phys.* **1999**, *1*, 437.
(32) Larson, S. A.; Widegren, J. A.; Falconer, J. L. *J. Catal.* **1995**, *157*, 611.
(33) Anbar, M.; Neta, P. *Int. J. Appl. Radiat. Isotopes* **1967**, *18*, 493.
(34) Nosaka, Y.; Nosaka, A.; *Nyuumon Hikari Shokubai*; Tokyo Tosho Press: Tokyo, 2004; Vol. 120 (in Japanese).

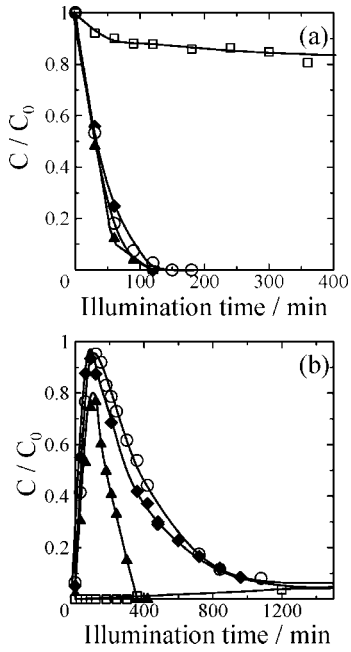

Figure 13. 2-Propanol and acetone concentration change during UV illumination: ○, $(TiO_2)_6$; ♦, $(PW_{12}/TiO_2)_6$; ▲, $(PW_{12}/TiO_2)_6$ covered with the PW_{12} layer; and □, $(PW_{12})_6$.

that of $(PW_{12})_2$, which suggests that the $(PW_{12})_6$ thin film absorbed 2-propanol, acetone, and the intermediate in the interlayer.

Figure 13b portrays the concentration change of acetone during UV illumination of $n = 6$ samples. Increasing layer thickness increased the acetone decomposition rate of hybrid films. Especially, the $(PW_{12}/TiO_2)_6$+PW_{12} sample exhibits a high acetone decomposition rate: all acetone was decomposed in 6 h. This trend differs from that of 2-propanol decomposition. The acetone decomposition rate depends on the layer thickness. This result indicates that the bottom or inner part of the $n = 6$ sample is also related to acetone decomposition. The whole sample will contribute to acetone decomposition, but in the case of 2-propanol decomposition, only the material near the surface contributes. The result may suggest that the relationship between the organic molecule diffusion rate into the layer and the photocatalytic decomposition rate affects the decomposition rate dependence on the layer thickness. However, we cannot discuss the difference between 2-propanol and acetone in detail using only these data because 2-propanol decomposition is a one-step reaction by one photon, and the acetone decomposition is a multistep reaction. Further investigation is required on this difference. The photocatalytic reaction in this film is not simple; it is related to the charge transfer between PW_{12} and TiO_2. Moreover, the top layer is expected to affect molecular adsorption and release behavior.

Figure 14 shows the 2-propanol concentration change during UV illumination without $\lambda > 400$ nm visible light. For hybrid films, 2-propanol decomposition and acetone generation were stopped after 1 h of illumination. On the other hand, the TiO_2 film maintained the same performance after cutting $\lambda > 400$ nm visible light. This result shows that hybrid thin films required visible light illumination for continuous decomposition reactions. Using the laser flashing method for the PW_{12}−TiO_2 system, Majima et al. demonstrated that PW_{12}^- reoxidation occurs rapidly when irradiated with visible light.[18] In their research, PW_{12}^- was excited by visible light and quickly reduced methyl viologen in water. In addition, PW_{12}^- reoxidation by O_2 is a thermodynamically disadvantageous reaction in the absence of H_2O. However, when PW_{12} was illuminated with visible light, it obtained a large reduction power and reduced O_2. The O_2 reduction rate should be low, and electron−hole recombination rate was increased when visible light was cut. Then, the decomposition reaction apparently stopped.

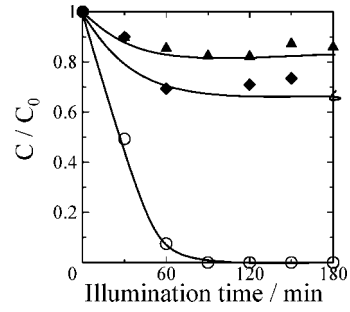

Figure 14. 2-Propanol concentration change when visible light > 400 nm was cut: ○, $(TiO_2)_6$; ♦, $(PW_{12}/TiO_2)_6$; and ▲, $(PW_{12}/TiO_2)_6$ covered with the PW_{12} layer.

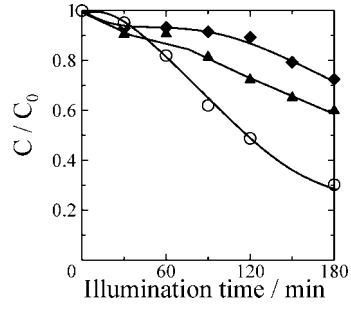

Figure 15. 2-Propanol concentration change when the UV < 330 nm was cut: ○, $(TiO_2)_6$; ♦, $(PW_{12}/TiO_2)_6$; and ▲, $(PW_{12}/TiO_2)_6$ covered with the PW_{12} layer.

Figure 15 depicts 2-propanol decomposition when the short wavelength UV (<330 nm) was cut. In this case, most of the light required to excite PW_{12} (<350 nm) was cut by the glass filter. Under this condition, PW_{12} was only slightly excited, but TiO_2 can be excited. The decomposition rate was decreased in all samples; however, its degree is more remarkable on hybrid films. This result indicates that PW_{12} excitation hastens 2-propanol decomposition. Excited PW_{12} acts as a better electron acceptor than ground-state PW_{12}.

Results of decomposition experiments show the redox mechanism. Figure 16 portrays the PW_{12}−TiO_2 redox system under both UV and visible light. Without a color filter, PW_{12} and TiO_2 were excited simultaneously. The holes by PW_{12} have strong oxidation power and trap electrons from TiO_2 effectively; consequently, it is reduced to PW_{12}^-, which absorbs visible light and obtains stronger reduction power than ground-state PW_{12}^-. It is sufficient to reduce O_2 in air. Ground state PW_{12} was regenerated by O_2 reduction. Because of effective electron consumption, TiO_2 charge recombination was prevented and photocatalytic activity was increased. The PW_{12} covered sample exhibited higher decomposition activity than that of PW_{12}/TiO_2 film because the O_2 reduction and TiO_2 oxidation balance are suitable to promote decomposition.

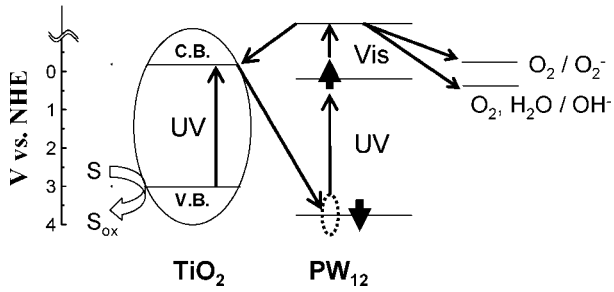

Figure 16. Energy diagram of the PW_{12}−TiO_2 system in air.

Because the reduction potential for O_2 is higher than that for PW_{12}^- when visible light was cut, PW_{12} reoxidation occurred only slightly in air. In contrast, when the light for PW_{12} excitation was cut, the ground-state PW_{12} acted as a scavenger. The ground-state PW_{12} acts as a weaker electron scavenger than excited PW_{12}. The reaction rate was expected to be lower than in the visible light illumination case. Water adsorbed on the films' surfaces will also play an important role for overall photocatalytic performance. The effect of water adsorption remains as a subject for future research.

The PW_{12}−TiO_2 system can use a wide range of light wavelengths for decomposition. A light source that has a large wavelength distribution, such as solar light, is advantageous. By changing the kind of HPA, the acceptor level and reaction behavior with O_2 should also be changed. For that reason, different light responsibility might appear.

For this study, we prepared the $(PW_{12}/TiO_2)_n$ hybrid films using layer-by-layer coating. Subsequently, we demonstrated that these films possess high photocatalytic activity against both 2-propanol and acetone. Actually, Keggin-type HPAs are known to decompose fluorocarbons in aqueous media. This material might also decompose gaseous fluorocarbon if optimization is attained.

IV. Conclusion

Using the layer-by-layer method, 12 tungsto(VI) phosphoric acid (PW_{12}) and TiO_2 hybrid thin films were prepared for this study. Both IR and UV−vis absorbance spectra indicated that alternative deposition occurred and that the PW_{12} Keggin structure was maintained after coating. For 2-propanol decomposition, 2-bilayer thin films (ca. 15 nm) exhibited higher decomposition rates than that of the control TiO_2 film. The photocatalytic decomposition activity depends on the number of bilayer coatings, the top coating, and organic compounds for decomposition. Simultaneous excitation of TiO_2 and PW_{12} by UV, along with illumination of visible light for the transition of PW_{12} to PW_{12}^-* are important mechanisms for the photocatalytic reaction in this system.

Acknowledgment. This work was supported in part by JSPS Research Fellowship No. H19-9009.

CM800167X